Journal of Pharmaceutical and Biomedical Analysis 265 (2025) 116995

Contents lists available at ScienceDirect

Journal of Pharmaceutical and Biomedical Analysis

journal homepage: www.journals.elsevier.com/journal-of-pharmaceutical-and-biomedical-analysis

Structure elucidation and quantification of the active pharmaceutical ingredient in a non-approved drug and in cat serum using QTRAP-MS/MS and ZenoTOF-MS/MS

Luke Tu [a,b], Jeannie Horak [a,b,*], Daniela Krentz [c], Katharina Zwicklbauer [c], Katrin Hartmann [c], Eveline Lescrinier [d], Martin Alberer [e], Ulrich von Both [e,f], Berthold Koletzko [a,b,*]

[a] Department of Pediatrics, Dr. von Hauner Children's Hospital, LMU Hospital, LMU Munich, Lindwurmstrasse 4, Munich D-80337, Germany
[b] German Center for Child and Adolescent Health, Munich, Germany
[c] LMU Small Animal Clinic, Centre for Clinical Veterinary Medicine, LMU Munich, Veterinaerstrasse 13, Munich D-80539, Germany
[d] Medical Chemistry, KU Leuven, Rega Institute for Medical Research, Leuven 3000, Belgium
[e] Division of Pediatric Infectious Diseases, Dr. von Hauner Children's Hospital, LMU Hospital, LMU Munich, Munich D-80337, Germany
[f] German Center for Infection Research (DZIF), Munich, Germany

ARTICLE INFO

Keywords:
Feline infectious peritonitis
Antiviral drug
Xraphconn
GS-441524
MRM-IDA-EPI scan
ZenoTOF
Electron activation dissociation

ABSTRACT

Feline infectious peritonitis (FIP) is a fatal systemic disease in cats caused by a feline coronavirus (FCoV). Recent studies have shown that Xraphconn, an unapproved veterinary drug, has significantly increased survival rates in cats with FIP. However, the lack of transparent information regarding the chemical structure and quantity of the active pharmaceutical ingredient (API) necessitates a thorough investigation of this drug. In this study, the API from Xraphconn's plant-based matrix was successfully isolated and purified using weak cation-exchange solid-phase extraction (WCX-SPE). Preliminary structure elucidation was conducted using mass spectra simulations, multiple reaction monitoring–information-dependent acquisition-enhanced product ion (MRM-IDA-EPI) scans from a 6500+ QTRAP-MS, and both collision-induced dissociation (CID) and electron-activated dissociation (EAD) fragmentation techniques with the ZenoTOF 7600. Conclusive structural identification of the Xraphconn API was achieved by ^{13}C and ^{1}H nuclear magnetic resonance spectroscopy. A 4-minute RP HPLC-MS/MS method was optimized to achieve satisfactory separation of the API peak from an isobaric contaminant. The limit of detection (LOD) and limit of quantification (LOQ) were established at 2.11 nM and 6.39 nM in water, and 7.21 nM and 21.84 nM in plasma, respectively. The intra- and inter-day accuracy was found to range between 96 % and 105 %, with a coefficient of variation (CV%) of $\leq$ 5.51 %. The API content was determined to be 21.56 $\pm$ 0.98 mg per tablet employing $^{13}C_5$-GS-441524 as an internal standard to account for potential matrix effects. The API concentration was measured in plasma and serum samples collected at four different time points from six treated cats.

1. Introduction

Feline Coronavirus (FCoV) is a common viral infection in cats. Like the highly transmissible severe acute respiratory syndrome coronavirus 2 (SARS-CoV-2) that caused the COVID-19 pandemic, FCoV is a member of the coronaviridae family [1]. It exists in two biotypes, the less virulent FCoV, is highly contagious but only causes mild symptoms. The other biotype, the FIP-associated virus, is the virulent biotype, caused by spontaneous mutation. Although the mutated variant is the source of infection in only a small percentage of infected cats, it can lead to the lethal disease feline infectious peritonitis (FIP) [2]. While FIP is recognized as one of the leading infectious causes of death in cats, the specific viral mutations responsible for the biotype switch and the pathogenesis of FIP are yet to be fully disclosed. Traditional treatment options such as immunomodulators or immunosuppressive agents only temporarily alleviate clinical symptoms, but all cats ultimately died [3].

* Corresponding authors at: Department of Pediatrics, Dr. von Hauner Children's Hospital, LMU Hospital, LMU Munich, Lindwurmstrasse 4, Munich D-80337, Germany.
E-mail addresses: Jeannie.Horak@med.uni-muenchen.de (J. Horak), Berthold.Koletzko@med.uni-muenchen.de, office.koletzko@med.lmu.de (B. Koletzko).

https://doi.org/10.1016/j.jpba.2025.116995
Received 26 March 2025; Received in revised form 22 May 2025; Accepted 26 May 2025
Available online 27 May 2025

Research has shown that antiviral drugs such as GS-441524 are effective in the treatment of FIP and achieve high remission rates [4]. One drug used in several studies that has been sold without approval by regulatory agencies is Xraphconn (Mutian Life Sciences Co. Ltd., Nantong, China) [5]. Xraphconn is a yellow film-coated tablet and described in the package insert as containing herbal constituents such as radix scrophulariae, platycodon grandiflorum, phyllostachys pubescens, forsythia suspense, and anemarrhena asphodeloides. One of its claimed active pharmaceutical ingredients (API) is MT-0901. However, Mutian, the manufacturer, has provided two distinct chemical formulations for MT-0901, both isomeric, but not identical to GS-441524. In addition to the unclear chemical structure of the API, also the API amount in the drug formulation is not reported.

Given these uncertainties, it seemed essential to explore reliable analytical methods for the identification and quantification of the API in Xraphconn. Multiple reaction monitoring–information-dependent acquisition-enhanced product ion (MRM–IDA–EPI) scanning on a hybrid triple quadrupole-linear ion trap (QqLIT or QTRAP) instrument is a cost-effective and accessible tool for a broad range of laboratories to generate mass spectra for compound verification and identification. QqLIT utilizes MRM as a preliminary survey scan, followed by IDA, which triggers the subsequent EPI scanning upon fulfillment of the predefined IDA criteria. During the EPI scan, fragmented ions are captured and temporally stored within the linear ion trap prior to their sequential release, which significantly enhances sensitivity and specificity, while facilitating the generation of high-quality MS/MS spectra [6]. Concerning its use and applicability, this technique was successfully applied for structure confirmation of adulterants in dietary supplements [7], characterization of drug metabolites [8], multi-target screening of drug compounds in serum and urine [9] as well as structure identification of eicosanoids in human plasma [10]. Naturally, the mass resolving power combined with higher mass accuracy of Orbitrap (OT) and quadrupole time-of-flight (QTOF) instruments provide a much broader applicability for drug and drug metabolite screening [11] as well as comprehensive untargeted metabolite and lipid profiling in biological samples [12]. Advanced features, like ion mobility [13], ultraviolet photodissociation (UVPD) [14], and electron-activated dissociation (EAD) [15], further enhance the structural insights achievable with these techniques, providing valuable information for molecule characterization and identification [16]. Furthermore, nuclear magnetic resonance (NMR) spectroscopy is a powerful analytical tool which provides detailed information about the chemical environment and connectivity of atoms within a molecule, making it especially valuable for structure elucidation [17].

Several analytical techniques are available for the quantification of antiviral drugs like GS-441524, including two-dimensional liquid chromatography-tandem mass spectrometry (2D-LC-MS/MS) [18], high-performance liquid chromatography with fluorescence detection [19], and LC-MS/MS methods with short gradient times [20,21].

In this study, the antiviral API from the drug formulation Xraphconn, which has a high content of plant matrix besides the API was successfully isolated. During the analysis, an impurity peak co-eluting with the API was discovered. Baseline separation of this isobaric impurity from the target analyte was achieved using an optimized 4-minute UHPLC-ESI-QTRAP-MS/MS method, employing a 5 cm Waters Cortecs T3 core-shell C18 column and 0.15 % formic acid (FA) in the mobile phase. To identify the API's chemical structure, computer-simulated mass spectra of potential candidates with mass spectra obtained from MRM-IDA-EPI scans of the isolated Xraphconn API was compared. Furthermore, the fragmentation patterns between the GS-441524 standard and the Xraphconn API were analyzed and compared using both low-resolution MS on the QTRAP 6500+ and high-resolution MS on the ZenoTOF 7600. In addition, ^{1}H and ^{13}C NMR were employed to obtain more in-depth chemical structure information. The optimized LC-MS/MS method was then applied for the quantification of the API content in Xraphconn tablets as well as in the blood samples of six Xraphconn-treated cats collected at four time points.

2. Experimental

2.1. Chemicals, standard solutions and consumables

LC-MS grade water, methanol (MeOH) and acetonitrile (ACN) as well as ammonium hydroxide (NH_4OH), hydrochloric acid (HCl), 6,7-dimethyl-2,3-di(2-pyridyl) quinoxaline (QX), 200 µL polymerase chain reaction (PCR) 96-well microplates (conical, skirted) from Axygen (Corning; AZ, USA) and 1.2 mL 96 deep-well plates (round bottom, low profile) from Brand were purchased from Sigma-Aldrich (Schnelldorf, Germany). Formic acid was from Carl ROTH (Karlsruhe, Germany). GS-441524 standard was purchased from ABCR (Karlsruhe, Germany) and the isotopically labelled internal standard $^{13}C_5$-GS-441524 was from Alsachim (Illkirch, France). Human control plasma level I and level II (CP-I and CP-II) from RECIPE (Munich, Germany) were prepared according to manufacturer instructions and pooled for use as quality control (QC).

The standard stock solutions, 10 mM GS-441524 and 2.5 mM $^{13}C_5$-GS-441524 were prepared in water and adjusted to a pH of 2 using 1 M HCl. The 5 mM QX stock solution was prepared in 5 % water in methanol. All subsequent dilutions were performed with water only.

Xraphconn tablets were purchased from Mutian Life Sciences Co. Ltd. (Figure S1).

The PCR microplate aluminum heat sealing foil, the HeatSealer S100 and the ThermoMixer C with well plate adapter were from Eppendorf (Wesseling, Germany). Polypropylene PCR microplate foil was from RatioLab (Dreieichen, Germany). The silica-based propyl carboxylic acid (PCA) weak cation exchange (WCX, 500 mg, 3 mL) solid phase extraction (SPE) cartridges and the 96-well polytetrafluoroethylene (PTFE) membrane filter plates (0.45 µm) were obtained from Macherey-Nagel (Dueren, Germany). The solid-phase-extraction (SPE) tube adapter for 1, 3 and 6 mL SPE tubes was purchased from Sigma Aldrich and the 10 mL syringes were from Becton Dickinson S.A. (Fraga, Spain). The vortexer was from IKA-Werke GmbH & Co. KG (Staufen, Germany). The balance PRACTUM64–1S (1 g - 0.01 mg) was obtained from Sartorius Lab Instruments GmbH & Co. KG (Goettingen, Germany). The centrifuge ROTINA 380 R (96-wellplates) and centrifuge MIKRO 22 R (1.5 mL and 2.0 mL microcentrifuge tubes) were from Andreas Hettich GmbH & Co. KG (Tuttlingen, Germany). The nitrogen generator NGM 22-LC/MS was from CMC Instruments GmbH (Eschborn, Germany). The nitrogen sample concentrator with Dri-Block DB100/3 heater, sample concentrator, PTFE coated needles and 96-well block thermostat for Dri-block were from Techne, purchased from VWR (Darmstadt, Germany).

2.2. Sample preparation

2.2.1. Isolation of GS-441524 from Xraphconn

A 200 mg Xraphconn tablet was weighed (348.66 mg ± 0.15 mg; n = 4) and ground to a fine light green powder in a 10 mL agate mortar with pestle. Four aliquots of 3–4 mg (Table S1) were weighed into 2 mL screw cap tubes and stored at −30°C prior to use. To each of the four aliquot tablet powders, 200 µL MeOH and 30 µL 2.5 mM $^{13}C_5$-GS-441524 were added as the internal quantification standard and vortexed for 2 min. Subsequently, 800 µL of water was added, along with 20 µL of 1 M HCl, in order to adjust the pH to a range of 2–3, with the objective of enhancing the solubility of the API. The extract was vortexed for another 2 min, left at room temperature for 5 min and centrifuged for 5 min at 13000 rpm. The supernatant 1 was pipetted into a 10 mL volumetric flask. The residue was twice extracted with 500 µL water plus 10 µL 1 M HCl for pH adjustment (supernatant 2), and a final extraction was performed with 1 mL water plus 20 µL 1 M HCl (supernatant 3). All supernatant solutions were pooled in the same 10 mL volumetric flask and volume adjustment was performed with water.

From this pooled extract, 100 µL was added to 900 µL water,

followed by pH adjustment with 0.05 % aqueous NH_4OH to a pH of 6–7. API purification was performed using WCX-SPE tubes. The SPE tubes were conditioned with 8 × 1 mL MeOH, and 8 × 1 mL water, before application of the diluted and pH adjusted Xraphconn extract. The API was eluted from the SPE cartridge with 2 × 1.2 mL 5 % FA in water directly into 2 mL screw cap tubes using a tube adapter in combination with a 10 mL syringe, which resulted in elution fraction A and B.

To both elution fractions of each of the four extract replicates, 45 µL 10 µM (0.45 nmol or 140.57 ng in water) 6,7-dimethyl-2,3-di(2-pyridyl) quinoxaline (QX) was added as an internal recovery standard. From these purified API solutions, 5 µL were added to 45 µL water in 200 µL 96-well microplates and analyzed via UHPLC-ESI-QTRAP-MS/MS.

2.2.2. Quantification of GS-441524 in Xraphconn

For the quantification of the API GS-441524 in the Xraphconn tablet extracts, the following seven calibrant solutions were prepared directly in the 200 µL 96 micro-well plate by addition of 5 µL of GS-441524 standard dilution 0.05, 0.1, 1, 5, 10, 25 and 50 µM GS-441524, to 45 µL 50 nM $^{13}C_5$-GS-441524 in water (Figure S2a).

For determination of the extraction efficiency, QX was used as the internal recovery standard for the quantification of $^{13}C_5$-GS-441524, which was added prior to extraction. The calibrant solutions for recovery yield determination were prepared directly in 200 µL 96 micro-well plates by addition of 5 µL of 0.05, 0.1, 0.25, 0.4, 0.5, 0.75 and 1 µM $^{13}C_5$-GS-441524 in water to 45 µL 50 nM QX in water (Figure S2b).

2.2.3. Cat plasma and serum samples collection

Plasma and serum samples were collected from cats treated for FIP with Xraphconn as described in detail by Krentz et al. [22]. Serum samples from six cats of the same cat breed were collected on day 0 (before treatment) and day 7 (after start of treatment), both before and 4 hours after drug administration as well as plasma samples collected on day 7 before and 4 hours after drug administration. All six cats received a daily dosage of 5 mg/kg body weight on an empty stomach. All blood samples were frozen at −80 °C on the day of collection and stored until analysis.

2.2.4. Cat plasma and serum samples preparation

The extraction procedure was conducted in a 1.2 mL 96 deep-well plate by pipetting 25 µL of cat plasma and serum sample as well as six human plasma QCs (spiked with 4.75 µM GS-441524) directly into 225 µL of a 50 nM $^{13}C_5$-GS-441524 internal standard solution in MeOH. Due to the weakened state of cats enrolled in this study, the available blood sample volumes were not sufficient to prepare and use pooled cat serum QCs. Hence, commercial human plasma was used instead. The well plate was covered with a PCR adhesive foil and left at 4 °C for 15 min followed by 15 min shaking at 600 rpm. The flocculent protein precipitate in MeOH was transferred with a 300 µL 12-channel pipette (ErgoONE from StarLab (Hamburg, Germany) into a 96-PTFE filter well plate, which was attached to a 1.2 mL 96-deep-well plate with adhesive tape. The PTFE filter plate plus deep-well plate construct was centrifuged at 2000 rpm for 20 min at 4 °C. 50 µL of serum and plasma extract samples, human plasma QCs, 10 calibrator solutions (0, 0.0025, 0.005, 0.01, 0.05, 0.1, 1, 5, 10, 25, 50 µM GS-441524 in human plasma), one internal standard (ISTD) blank and one system blank (water) were pipetted into a 200 µL 96-micro-well plate. After solvent evaporation at 30°C with flowing nitrogen, 50 µL 0.15 % FA in water was added to each well. The well plate was covered with an aluminum heat sealing foil, shaken at 25 °C and 600 rpm for 20 min and stored at −30 °C prior to analysis. Before UHPLC-ESI-QTRAP-MS/MS analysis, the sample analysis well plate was shaken for 20 min at 25 °C and 600 rpm.

2.3. Instrumentation and methods

UHPLC-ESI-QTRAP-MS/MS measurements were performed on an Agilent 1290 UHPLC system comprised of a binary pump (G1720A), 1290 multisampler (G7167B) for 8 well plates and a temperature-controlled column oven (G7116B) from Agilent Technologies (Waldbronn, Germany) coupled to a QTRAP 6500+ hybrid MS from Sciex (Concord, Ontario, Canada) with Turbo-V ion source operated in positive electrospray ionization (ESI) mode. High-resolution MS/MS experiments were performed on ZenoTOF 7600 coupled with ExionLC from Sciex (Darmstadt, Germany) in CID and EAD modes to study the structure of API and potential impurities.

2.3.1. Chromatographic separation

Reversed phase separation was performed on a CORTECS UHPLC T3 core-shell column (2.1 mm×50 mm column; 1.6 µm particle size) with VanGuard pre-column from Waters GmbH (Eschborn, Germany) using 0.15 % formic acid (FA) in water as mobile phase A (MP-A) and 0.15 % FA in ACN as MP-B at a flow rate of 400 µL/min, a column temperature of 40°C and an injection volume of 2 µL. Gradient elution was applied: 0–0.30 min isocratic at 5 % MP-B; 0.30–0.35 min from 5 % to 30 % MP-B; to 1.50 min from 30 % to 70 % MP-B; to 1.80 min from 70 % to 90 % MP-B, isocratic from 1.80 min to 2.80 min at 90 % MP-B and re-equilibration at 2.90–4.00 min at 5 % MP-B. Note that FA concentrations of 0.05, 0.1 and 0.15 % were investigated to achieve separation from a co-eluting impurity peak at 0.05 % FA in MP-A and MP-B.

2.3.2. MRM-IDA-EPI for API structure elucidation

To obtain the MS-fragmentation pattern of the API extracted from the tablet, multiple reaction monitoring information dependent acquisition enhanced product ion scan (MRM-IDA-EPI) experiments were performed on a QTRAP 6500+ MS instrument. The MRM survey scan was conducted with a curtain gas (CUR) of 30 psi, collision gas medium, ion source gas 1 (GS1) 40 psi, GS2 40 psi, declustering potential (DP) 100 V, entrance potential (EP) 10 V, collision exit potential (CXP) of 10 V, ion spray voltage (IS) of 4500 V and a source temperature (TEMP) of 400 °C. The MRM settings for GS-441524 in positive ionization mode were Q1 *m/z* 292.1, Q3 *m/z* 163.1 and dwell time 20 msec. For IDA, *m/z* 292.1 was placed in the inclusion list for fragmentation at the retention time of GS-441524 at 1 min. In addition, IDA was performed for two high intensity peaks, for ions higher *m/z* 70 and smaller *m/z* 1000, which exceeds 500 cps. Former target ions were never excluded and mass tolerance was set to 250 mDa. EPI was performed with 2 experiments using a scan rate of 10000 Da/s. The MRM-IDA-EPI experiments for API extracted from Xraphconn and the commercial GS-441524 standard were performed at four different collision energies (CE): 40 V, 50 V, 60 V and 80 V. For this experiment 0.05 % FA in water (MP-A) and 0.05 % FA in ACN (MP-B) were used [21].

2.3.3. Structure elucidation of API and impurity using ZenoTOF-MS

Chromatographic separation was performed using a ExionLC AD system, with the column and LC method as detailed in 2.3.1. Mass spectrometry was conducted on a ZenoTOF mass spectrometer, operated in positive ion mode. The ion source parameters were set to CUR at 35 psi, GS1 at 40 psi, GS2 at 50 psi, IS at 5500 V, and TEM at 500 °C, with the CAD gas set to 7 psi. A TOF MS scan was conducted over the mass range of *m/z* 100–1000 with a CE of 10 V and a DP of 80 V. Product ion scans in tandem mass spectrometry were conducted using two fragmentation techniques: CID and EAD. The CID experiment targeted the precursor ion at *m/z* 292.10 (or *m/z* 297.10 for the internal standard $^{13}C_5$-GS-441524) within a mass range of *m/z* 40.0–300.0, with a CE of 40 V and DP of 60 V. The EAD experiment analyzed the same precursor ions with an electron kinetic energy of 12 eV and used a mass range of *m/z* 40–300 with an accumulation time of 0.105 seconds, with CE and DP set to 10 V and 60 V, respectively. Data acquisition for all experiments was conducted over a 4-minute period.

2.3.4. NMR analysis for API structure elucidation

The NMR sample was prepared and analyzed by NMR using a Bruker Avance II 600 MHz at 293 K equipped with 5 mm TCI cryoprobe as

previously described [22]. The HOD signal was suppressed by applying pre-saturation during a relaxation delay for 1 second in proton detected 1- and 2-dimensional spectra. Natural abundance [^{1}H, ^{13}C] heteronuclear single quantum coherence (HSQC) [23] was recorded with sensitivity enhancement and gradient coherence selection optimized for selection of CH groups in the sugar part of the nucleoside ($^{1}J_{CH}$ = 150 Hz) using 16 scans and 512/4096 complex data points and 120/10 ppm spectral widths in t1 and t2, respectively. A separate natural abundance [^{1}H,^{13}C]-HSQC was measured to determine the remaining ^{1}H–^{13}C correlations in the nucleobase. It was optimized for selection of aromatic CH groups ($^{1}J_{CH}$ = 180 Hz) using 16 scans and 128/4096 complex data points and 60/10 ppm spectral widths in t1 and t2, respectively. The natural abundance [^{1}H, ^{13}C] heteronuclear multiple bond correlation (HMBC) [24] was recorded using 64 scans and 215/4096 complex data points and 160/10 ppm spectral widths in t1 and t2, respectively ($^{1}J_{CH}$ = 200 Hz and $^{3}J_{CH}$ = 8 Hz).

2.3.5. Method validation

The matrix effect (ME), recovery (RE), and process efficiency (PE) of GS-441524 were evaluated using a commercial human control plasma as a surrogate matrix. Three concentration levels of GS-441524 at the lower limit of quantification (LLOQ), medium (Mid) and high (High) concentration, 0.025 μM, 25 μM, and 50 μM, respectively, were spiked to human plasma QC. The assessment was conducted using three sets of samples: i) neat solutions, ii) post-spiked samples (GS-441524 added to plasma extracts after extraction), and iii) pre-spiked samples (GS-441524 added to plasma samples prior to extraction). Each set was prepared in quadruplicate. The calculation of ME, RE and PE were conducted as outlined by Matuszewski et al. [25]. Intra-day and inter-day accuracy and precision were determined by spiking the control plasma mixture with GS-441524 at the same three concentration levels (0.025 μM, 25 μM, and 50 μM), with measurements taken on three separate days. According to the ICH Q2 (R1) guideline, the lower limit of detection (LOD) and lower limit of quantification (LOQ) for GS-441524 were established in both neat solution and plasma, calculated with 3.3 x and 10 x the standard deviation of the response of the y-intercept divided by the slope of the calibration curve [26].

2.3.6. Quantification of GS-441524

Quantitative analysis of GS-441524 in drug tablets as well as serum or plasma samples were performed on the QTRAP 6500+ using MRM, employing the following optimized ion source parameters: CUR 30 psi, GS1 50 psi, GS2 65 psi, IS 5500 V and TEM 600°C. Optimized chemical and source parameters for the chosen quantifier and qualifier fragment ions of GS-441524, $^{13}C_5$-GS-441524 and QX are listed in Table 1.

2.3.7. Software information

Analyst 1.7 with Analyst Device Driver (QTRAP 6500+) and Sciex OS (ZenoTOF 7600) were utilized for data acquisition, Sciex OS for qualitative data processing and MultiQuant™ 3.0.3 for quantitative data analysis. These software packages were from Sciex. For data visualization (mass spectra and plots), R version 4.1.0 and R-Studio (The Comprehensive R Archive Network, CRAN, Vienna, Austria) were used in combination with the R-packages readxl, dplyr and ggplot2.

2.3.8. Mass spectra simulation

Mass spectra simulation was performed via Competitive Fragmentation Modeling for Metabolite Identification (CFM-ID) (https://cfmid.wishartlab.com/) [27]. This online tool generates ESI-MS/MS mass spectra from target compounds of interest, for which no commercial standards are available. Parent compound structures were uploaded in international chemical identifier (InChI) or simplified molecular input line entry system (SMILES) format. The ESI spectra type in positive ionization mode was employed for the adduct type $[M+H]^{+}$. Mass spectra with list of fragment ions with their chemical structures were generated for multiple collision energies (Supporting Information). Information about the isobaric compounds, which are structurally related to GS-441524 together with their characteristic fragment ion structures is shown in Fig. 1.

3. Results and discussion

3.1. Structure elucidation of the API in Xraphconn on a QTRAP 6500+

The company Mutian Biotechnology Co. Ltd. has claimed that the API in Xraphconn is ((2S,3 R,4 R,5 R)-2-(4-aminopyrrolo[2,1-*f*]-[1,2,4]-triazin-7-yl)-3,4,5-trihydroxytetrahydro-2H-pyran-2-carbonitrile), referred to as MT-0901 in their package insert (Figure S1). However, earlier formulations of a similar antiviral product for treating FIP have shown different chemical structures for MT-0901. To avoid confusion, the originally described API structure will be referred to as MT-0901, while the API in Xraphconn' under investigation, will be referred to as Xraphconn. Their chemical structures are shown in Fig. 1. Since Xraphconn is not a regulatory authority approved drug formulation and the chemical structure of the API MT-0901 is unclear, an extraction and purification process (Fig. 2) to isolate the Xraphconn API for in-depth structure elucidation via LC-MS/MS was developed. During a patent and literature search, it was found that the original structure of MT-0901 as well as that of the isobaric compound GS-441524 were covered by an existing patent [28,29], while the chemical structure of Xraphconn API was not included in any patent or literature reference. After a failed patent application of the actual GS-441524 chemical structure [30], a patent application for the Xraphconn API structure was submitted by Nantong Weishun Biotechnology Co., LTD [31,32]. In this context, three potential structural API candidates, namely the Xraphconn API as described by the manufacturer, MT-0901, and GS-441524 were investigated. Due to its structural similarity and isobaric nature to these candidates, vengicide (toyocamycin) was also included.

Concerning their structural differences, MT-0901, GS-441524, and vengicide have a modified ribose ring known as 2-(hydroxymethyl) tetrahydrofuran-3,4-diol incorporate, which is also an integral part of the nucleoside structure.

In both, MT-0901 and GS-441524, the pyrrolo-[2,1-f]-[1,2,4]-triazin-4-amine moiety is attached to position 1 of the modified ribose ring. The distinguishing feature between these two compounds lies in the position of the cyano group. Specifically, in GS-441524, the cyano group is located at the 1′ position of the ribose ring, whereas in MT-0901, it is bonded to the 4′ position. In case of vengicide, an aminopyrrolo-[2,3-d]-pyrimidine moiety, complete with a cyano group, is affixed to the modified ribose ring. In Xraphconn API, the

Table 1
Compound-specific MS parameters for quantification (quanti) and compound identification (quali).

Compound	Application	Q1 *[m/z]*	Q3 *[m/z]*	RT *[min]*	DP *[V]*	CE *[V]*	CXP *[V]*
GS−441524_quanti	Standard	292.1	163.1	0.76	80	35	20
GS−441524_quali		292.1	172.1	0.76	80	35	20
$^{13}C_5$-GS−441524_quanti	Internal Standard	297.1	164.2	0.76	80	50	20
$^{13}C_5$-GS−441524_quali		297.1	148.1	0.76	80	50	20
QX_quanti	Recovery Standard	313.2	78.5	1.63	80	50	20
QX_quali		313.2	246.2	1.63	80	50	20

Theoretical [M+H]⁺ [m/z]	Experimental [M+H]⁺ [m/z]	Δ m/z [m/z]	GS-441524	MT-0901	Xraphconn	Vengicide
292.1040	292.08	-0.02	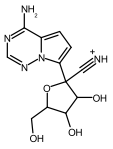	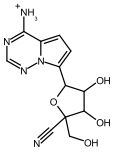	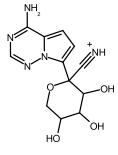 „proposed structure“	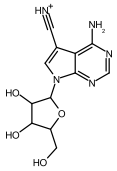
192.0880	192.12	0.03	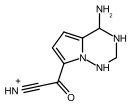	X	Not found, but could be present	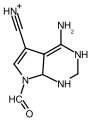
190.0723	190.08	0.01	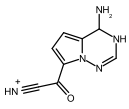	X	Not found, but could be present	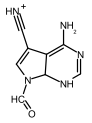
188.0567	188.04	-0.02	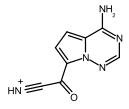	X	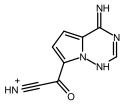	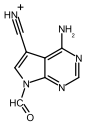
174.0774	174.00	-0.08	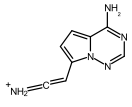	X	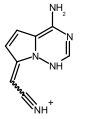	Not found
172.0618	172.08	0.02	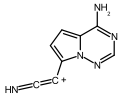	X	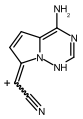	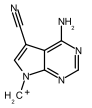
157.0509	157.08	0.03	Not found, but could be present	X	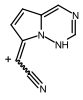	Not found
157.0509	Not found	Not found	Not found, but could be present	X	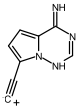	Not found

Fig. 1. Comparison of the compound characteristic fragments for the isobaric drug substances GS-441524, MT-0901, Xraphconn API and Vengicide with $[M+H]^+$ *m/z* 292.1040. All fragment structures and *m/z* values were obtained through mass spectra simulation. The theoretical *m/z* values are from GS-441524, while the experimental *m/z* are from the Xraphconn API extract. Measurements were performed on a UHPLC-ESI-QTRAP-MS/MS in positive ionization mode using Multiple Reaction Monitoring with Information Dependent Acquisition combined with an Enhanced Product Ion scan (MRM-IDA-EPI) using a collision energy of 50 V.

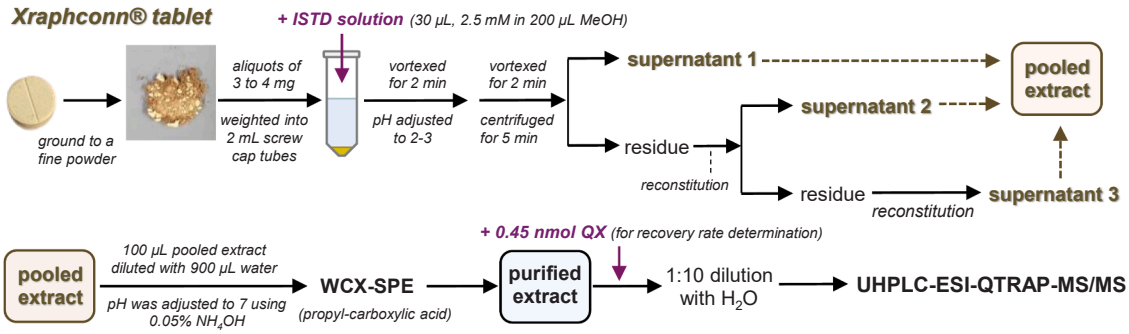

Fig. 2. API extraction and purification procedure for 3–4 mg ground Xraphconn tablet powder using a weak cation exchange solid phase extraction (WCX-SPE) cartridge. The internal standard (ISTD) $^{13}C_5$-GS-441524 was added to the crude extract solution, while the recovery standard QX was added to the purified extract after WCX-SPE clean-up and before UHPLC-ESI-QTRAP-MS/MS analysis.

tetrahydro-2H-pyran-3,4,5-triol ring and the cyano group are bound at position 6 to pyrrolo-[2,1-f]-[1,2,4]-triazin-4-amine.

As the proposed Xraphconn API and MT-0901 API are not commercially available, a mass spectra simulation was conducted for the four possible API molecules (Fig. 1). The characteristic fragments of Xraphconn, MT-0901, Vengicide, and GS-441524 were generated using CFM-ID [27] mass spectra simulation and compared in Fig. 1. The analysis revealed that the different positioning of the cyano group in MT-0901 prevents the formation of fragmentation ions identical to those in the Xraphconn API extract, allowing us to exclude MT-0901 as a candidate structure (Supporting Information). In contrast, both the manufacturer's proposed API structure and GS-441524 closely matched the fragmentation pattern of the Xraphconn API extract. Given the availability of commercial GS-441524 standard, a more detailed comparison was conducted. Mass spectra generated at four different CE settings using MRM-IDA-EPI scans on a QTRAP 6500+ instrument showed very similar fragmentation patterns for the Xraphconn API (Figure S3a) and GS-441524 (Figure S3b), with only slight variations in peak intensities observed.

While the measured and the CFM-ID computer simulated MS/MS mass spectra could verify the correct position of the cyano group in the Xraphconn API, it was nonetheless not possible to clearly distinguish the ribofuranose ring of GS-441524 from a ribopyranose ring in the specified Xraphconn API structure by LC-MS/MS alone, without co-analyzing the actual Xraphconn API standard under identical MS instrument settings. Therefore, further analytical investigations were necessary.

3.2. LC MS/MS method optimization for impurity peak removal

During preliminary structure elucidation experiments using 0.05 % FA in both mobile phases, MP-A and MP-B [21], a pronounced shoulder at the base of the chromatographic API peak of the GS-441524 standard was observed. Unexpectedly, this impurity shoulder was present in the extracted ion chromatograms (XIC) of the commercial GS-441524 standard as well as the XICs of the Xraphconn API extract and blood samples of Xraphconn treated cats. In order to obtain accurate quantitative results for the subsequent experiments, namely the quantification of the API content in the plant matrix rich Xraphconn formulation (Figure S1) as well as in blood samples of Xraphconn treated cats, this isobaric impurity peak had to be baseline separated from the analyte peak.

After investigating the influence of gradient settings, mobile phase (MP) composition and MP additive type, an increase in FA concentration in both, MP-A and MP-B, from 0.05 % to 0.15 % FA led to the separation of the impurity peak from the API peak (Fig. 3a) by decreasing the retention time of GS-441524 from 0.94 min to 0.77 min, while the impurity peak remained at 1.00 min and the QX recovery standard eluted at 1.64 min (Fig. 3b). Including column re-equilibration, the resulting LC-MS/MS method was only 4 min long.

3.3. ZenoTOF CID and EAD analysis of API and impurity

To gain further insight into the structural identity of the API and the impurity peak, additional measurements were conducted using the ZenoTOF 7600 HR-MS instrument. This instrument not only performs CID fragmentation but also generates EAD spectra, which ought to be unique for individual compounds and very different to CID generated mass spectra. Fig. 4a shows the XICs for the Xraphconn API extract and the GS-441524 standard, followed by their respective CID (Fig. 4b) and EAD spectra (Fig. 4c) for both the API and isobaric impurity peaks. The CID spectra of the Xraphconn API extract and GS-441524 standard were highly similar to each other and to their low-resolution MRM-IDA-EPI mass spectra (Figure S3). While CID spectra of the impurity peaks had similar fragment *m/z* values, their fragmentation patterns differed slightly. In the EAD spectra (Fig. 4c), the fragment masses for the Xraphconn API extract, GS-441524 standard, and impurity peaks were closely matched, but EAD fragmentation patterns of the impurity peaks were more similar to each other than to their respective APIs.

Fig. 5 compares the fragmentation patterns and relative fragment intensities of GS-441524 and the Xraphconn API in the CID- and EAD-induced mass spectra. Analysis of the CID and EAD fragment peaks, as proposed by the Sciex OS software, confirmed the presence of the heterocyclic "4-aminopyrrolo[2,1-*f*][1,2,4]triazin-7-yl" moiety. However, no specific fragment could be identified to distinguish between a ribopyranose or ribofuranose ring in the Xraphconn API. Despite the remarkable similarity in the CID and EAD fragment patterns between GS-441524 and the Xraphconn API, it could not be conclusively determined that the Xraphconn API is GS-441524 solely based on mass spectrometry.

3.4. NMR analysis of the API

To obtain more conclusive structural information and validate our findings by mass spectrometry, additional ^{13}C and ^{1}H NMR

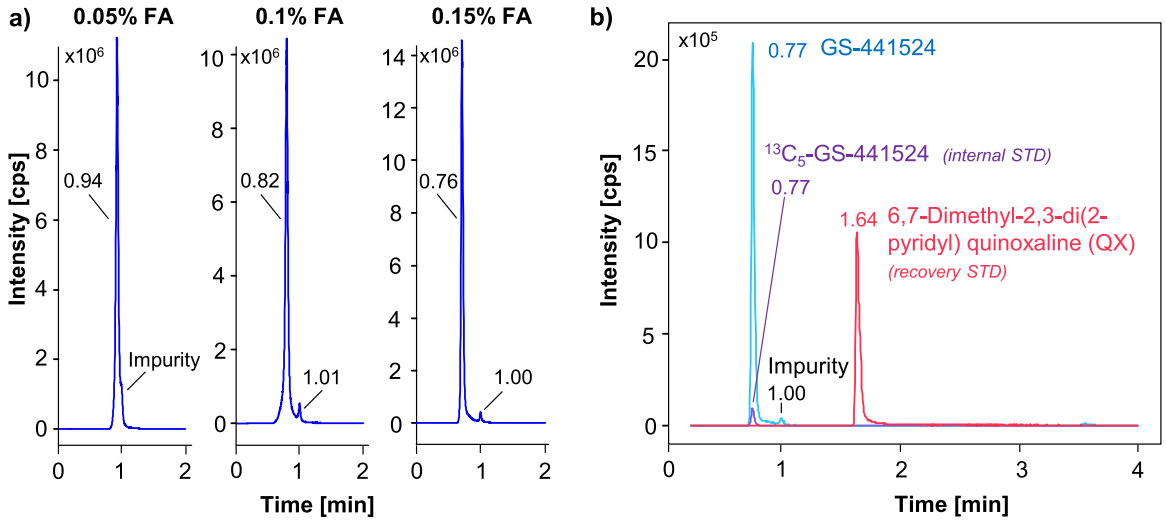

Fig. 3. a) Extracted ion chromatograms (XICs) for *m/z* 292.1 analyzed with MRM in positive mode on a UHPLC-ESI-QTRAP-MS/MS show the chromatographic separation of the isobaric impurity peak from GS-441524 with increasing concentration of formic acid (FA) from 0.05 % to 0.1 % and 0.15 %. b) Overlayed XICs for GS-441524 (*m/z* 292.1), the internal standard $^{13}C_5$-GS-441524 (*m/z* 297.1) and the recovery internal standard QX (*m/z* 313.2).

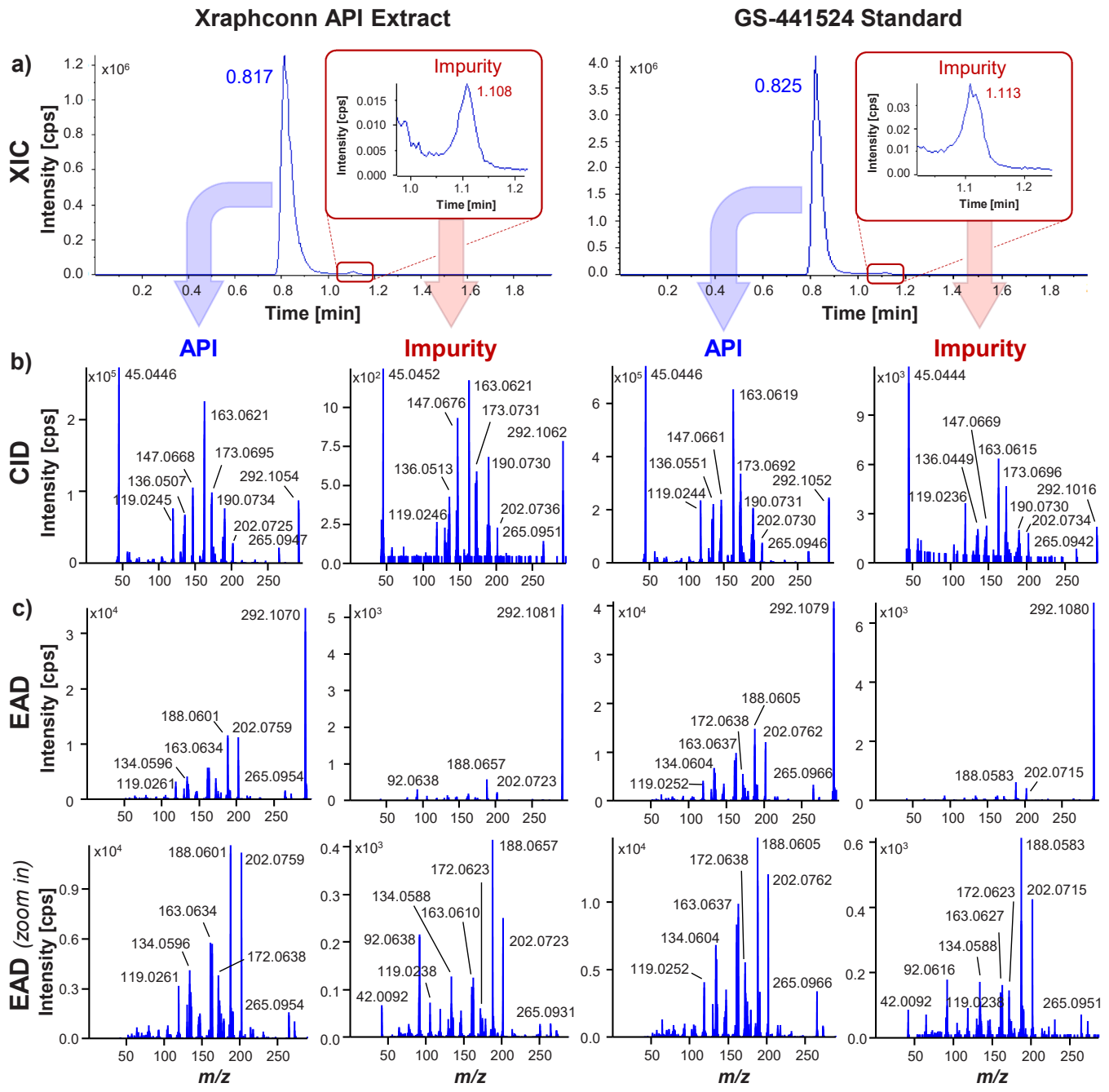

Fig. 4. a) XIC from $[M+H]^+$ with *m/z* 292.1040 generated on the Zeno TOF 7600 system for the purified Xraphconn API extract and for the GS-441524 standard with a zoom-in of their isobaric impurity peaks at 1.11 min, b) CID mass spectra for the respective API and their impurity, and c) shows their EAD mass spectra with an additional zoom-in to better visualize their EAD fragmentation patterns.

measurements were conducted on the isolated Xraphconn API. As shown in Figure S4, all ^{13}C and ^{1}H chemical shifts of the API in Xraphconn correspond to those reported for GS-441524 [33]. The furanose ring is confirmed by the presence of HO5' with correlation spectroscopy (COSY) cross peaks to both H5' protons and absence of HO4', while for a pyranose ring the opposite is expected. Regarding the isobaric impurity eluting at 1.11 min in Fig. 4, the available quantity of about 3.4 % area of the main API peak was insufficient for an in-depth structural elucidation. However, based on a previous report by Chen et al. [34], an α-anomeric diastereomer at the C1' position (CN isomer) could have been formed as a byproduct of the industrial production process of GS-441524, which led us to believe that the isobaric impurity may indeed be the diastereomer of GS-441524.

3.5. Method validation

The assessment results of ME, RE, and PE are presented in Table 2. The RE, determined from spiked human plasma QCs across the lowest, medium, and high GS-441524 calibration standard concentrations, exhibited a consistent range of 85.6–87.7 %, which are indicative for the reliability and stability of the extraction method employed. Notably, the ME values from 68.2 % to 73.3 % might suggest the presence of an ion suppression effect. Given that quantification relied on the peak area ratio of the analyte to the internal standard rather than solely on analyte peak areas, internal standard normalized matrix factor was also calculated and evaluated [26].

The internal standard normalized matrix factors, which ranged from

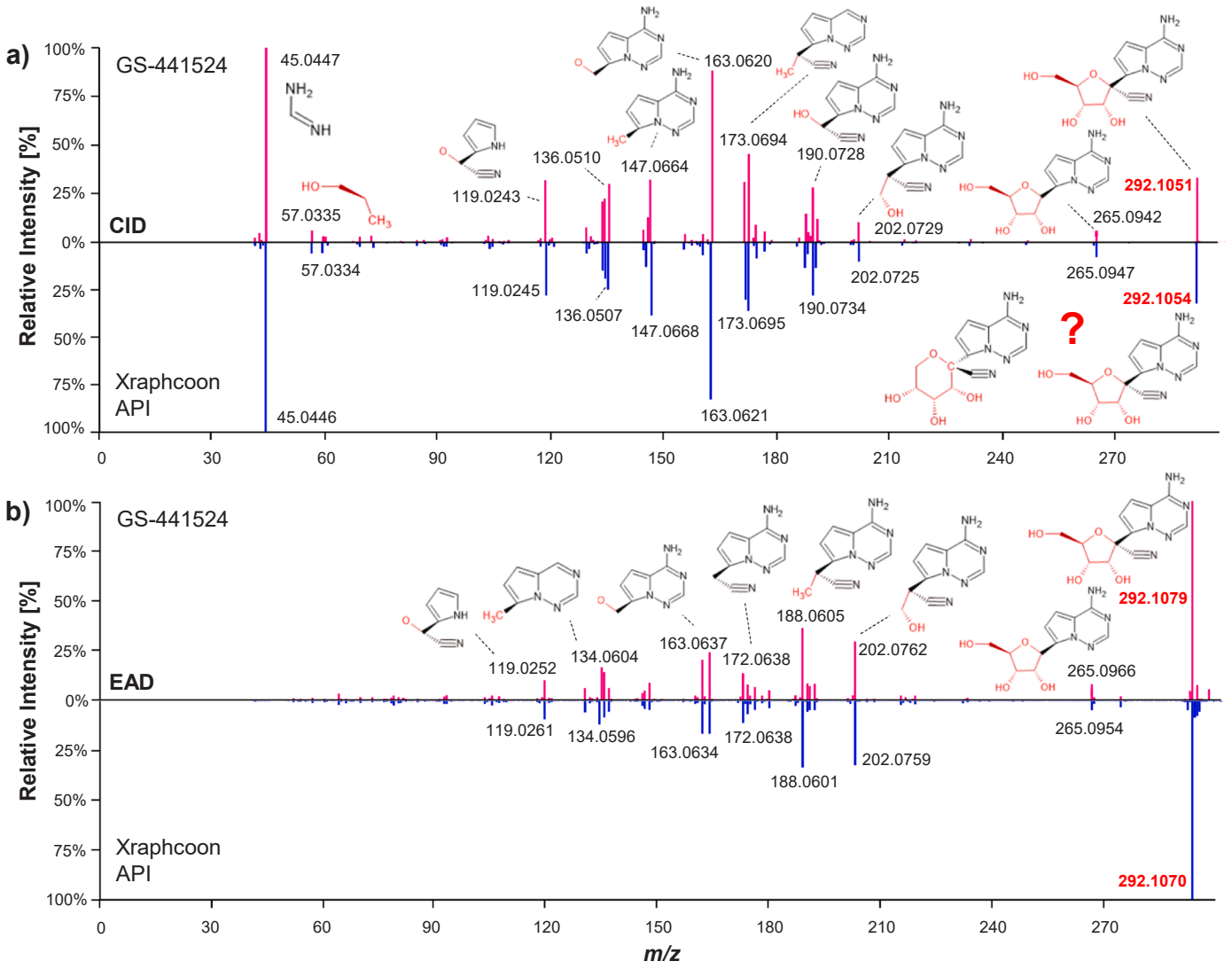

Fig. 5. a) CID and b) EAD fragmentation pattern of the API extracted from Xraphconn and the GS-441524 standard, generated on a ZenoTOF 7600 system.

Table 2
Matrix effect (ME), recovery rate (RE) and process efficiency (PE) plus accuracy and precision of QC_{LLOQ}, QC_{Mid} and QC_{ULOQ} (n = 4).

				Intra-day		*Inter-day*	
	ME	**RE**	**PE**	**Accuracy**	**Precision**	**Accuracy**	**Precision**
	[%]	*[%]*	*[%]*	*[%]*	*[%]*	*[%]*	*[%]*
QC_{LLOQ}	68.2 ± 8.1	85.9 ± 3.9	62.4 ± 7.9	96.15	1.87	99.97	2.87
QC_{Mid}	74 ± 1.7	87.7 ± 3.6	63.7 ± 6.5	103.32	0.10	108.17	5.51
QC_{ULOQ}	73.7 ± 1.5	85.6 ± 3.8	63.1 ± 3.4	104.13	1.53	102.34	1.43

0.9571 to 0.9887, demonstrated the effectiveness of the internal standard in compensating for matrix effects. The LOD and LOQ in neat solution was determined as 2.11 nM and 6.39 nM, respectively, while in plasma, they were 7.21 nM and 21.84 nM. Excellent linearity for GS-441524 was observed within the concentration range of 0.01 μM to 50 μM, with an R^2 value exceeding 0.9990. To assess a possible carry-over effect, the highest calibrator solution was spiked to plasma was injected four times consecutively, followed by subsequent injections of one blank plasma sample. This analysis sequence was replicated over three separate days. The percentage of GS-441524 carryover was deemed acceptable, falling within ± 20 % across three days (17.68 %, 15.4 %, and 19.61 %). Furthermore, for $^{13}C_5$-GS-441524, carryover percentages were consistently below 5 % (0.09 %, 0.14 %, and 0.04 %). Intra-day and inter-day precisions and accuracies were also assessed on three different days (Table 2). Precisions remained below 5.51 % in both, intra-day and inter-day experiments. In addition, accuracies within 96–105 % illustrated nicely the accuracy and reproducibility of this analytical method.

3.6. Quantification of GS-441524 in Xraphconn

In the process of extracting the API, methanol was utilized as the solvent. The solubility of GS-441524 was enhanced by adjusting the pH to a range of 2–3 using concentrated hydrochloric acid. In preliminary experiments involving the analysis of the crude API extract from the complex plant-based background components of Xraphconn, challenges such as low sensitivity to the target compound, significant carry-over, and contamination in LC-MS analyses were encountered, which made

accurate API quantification not feasible. In order to not only extract, but also purify the extracted API from the complex matrix, WCX-SPE was applied. The retained API were subsequently eluted using 5 % formic acid in water. The purified API was quantified using targeted QTRAP-MS, revealing the presence of 21.56 ± 0.98 mg of API in the Xraphconn tablet (n = 3), as detailed in Table S2. The weight of the Xraphconn tablet was determined to be 348.66 ± 0.15 mg, as opposed to the 200 mg stated in the product insert.

To prevent potential bias caused by instrument drift or degradation throughout the analysis, the calibration solutions for quantification and recovery rate determination were measured both before and after analyzing the tablet extracts. As shown in Figure S2a and FigureS2b, the two calibration curves overlap very well. Furthermore, the absence of carry-over for the purified API extract was confirmed by injecting system blanks (water) after each calibration standard and sample injection. The recovery rate was established using the recovery standard QX, which was added after solid-phase extraction, but before LC-MS analysis. This standard, unaffected by extraction losses, enabled accurate assessment of the internal standard's recovery by correcting for differences in response factors potentially arising from the purified API extract matrix. In this context, the calibration curves were constructed by plotting the peak area ratio of $^{13}C_5$-GS-441524 to QX against their employed weight ratio. An average recovery rate of 89.4 % was achieved.

3.7. Quantification of GS-441524 in cat plasma and serum

Thirty-six blood samples collected from six cats at four time points were analyzed. To ensure consistency and detect technical errors, all serum and plasma samples were analyzed in a randomized order and accompanied by six QCs.

In addition, after each sample, one internal standard blank injection was conducted to identify potential carryover induced by cat serum or plasma samples with unexpectedly high API content. Subsequent examination of all measurement data revealed no evidence of carryover. As shown in Fig. 6, prior to drug administration on day 0, none of the serum samples exhibited detectable levels of the API. However, four hours post-administration, a significant increase in API concentration was observed. Despite inter-individual variability among the six treated cats, all API concentrations remained within the range extending from 1.5 x the interquartile range (IQR) below the first quartile (Q1) to 1.5 x IQR above the third quartile (Q3), with no extreme outliers detected for timepoint d0–4h. On day 7, following daily drug administration, API was still detectable in all serum samples before dosing. Four hours post-treatment, API concentrations increased, with the median value being comparable to that observed on day 0. However, one serum sample on day 7 exhibited a markedly elevated API concentration, exceeding the median value by more than twofold. Additionally, API concentrations were measured in plasma samples on day 7, both before and after drug administration. The plasma sample from the same cat showed a similarly high API concentration after drug treatment compared to other cats, with serum and plasma levels closely matching. This consistency indicates that the elevated concentration had a biological cause and is not a technical outlier. As shown in Fig. 6, the plasma API concentrations across all six cats closely mirrored those observed in the corresponding serum samples, confirming thereby that serum as well as plasma samples can be reproducibly analyzed for GS-441524.

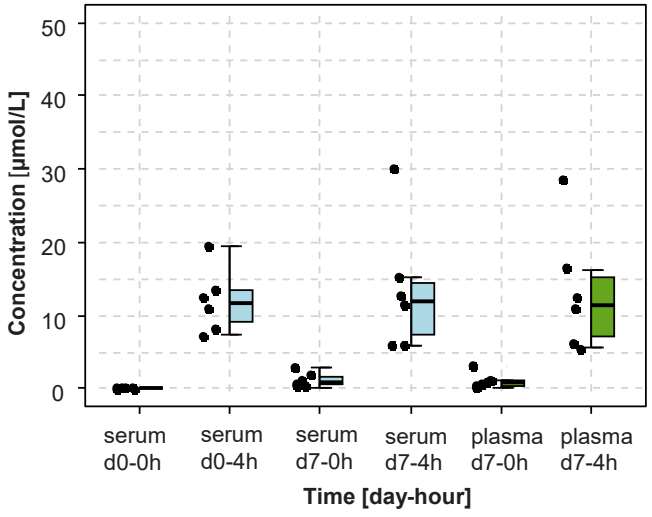

Fig. 6. Quantification results for the six investigated cat serum and plasma samples collected over a duration of 7 days (d). Sample collection on d0–0h and d7–0h were performed before drug administration, while sample collection d0–4h and d7–4h were performed 4 hours (h) after drug administration by the clinical study team.

4. Conclusions

In this study, a comprehensive analytical method to extract and isolate the Xraphconn API from its complex plant-based background matrix was developed, achieving recovery rates of 85.6–87.7 %. A 4-minute UHPLC-ESI-QTRAP-MS/MS method baseline separated an isobaric impurity from the main API peak. To determine the chemical structure of the isolated API, the performance of two different types of mass spectrometers, namely a low-resolution QTRAP 6500+ using MRM-IDA-EPI and a high-resolution ZenoTOF 7600 using CID and EAD for API molecule fragmentation were compared. Fragmentation patterns of the Xraphconn API were examined in relation to the commercially available GS-441524 and $^{13}C_5$ GS-441524 standards. While mass spectrometry confirmed the presence of the 4-aminopyrrolo[2,1-*f*][1,2,4] triazin-7-yl moiety in the Xraphconn API, it could not determine whether the attached ring was ribopyranose or ribofuranose. This limitation highlighted the need for complementary techniques like NMR, which confirmed the Xraphconn API as GS-441524. The API content in Xraphconn tablets was determined to be 21.56 ± 0.98 mg per 348.66 ± 0.15 mg tablet, equivalent to 6.18 mg of API per 100 mg of tablet. Quantitative analysis of blood samples from Xraphconn-treated cats revealed consistent API concentrations in both serum and plasma, with a clear trend observed between pre- and post-administration samples. However, considerable interindividual variability in API concentrations was observed, potentially influenced by various physiological and pathological factors such as body weight, age, FIP-related symptoms, and disease severity, which can affect drug absorption, distribution, metabolism, and clearance. Additionally, treatment-related adverse effects, including elevated liver enzyme activity and lymphocytosis, may further impact drug metabolism and clearance. For instance, a pharmacokinetic study in humans demonstrated that renal dysfunction can significantly alter plasma concentrations of GS-441524 [35]. These considerations clearly highlight the need for a comprehensive characterization of the pharmacokinetics of GS-441524 in treated cats to optimize dosing strategies and enhance therapeutic outcomes.

CRediT authorship contribution statement

Luke Tu: Methodology, Formal Analysis, Investigation, Validation, Visualization, Writing – original draft, Writing – review & editing. **Jeannie Horak:** Conceptualization, Methodology, Investigation, Project Administration, Supervision, Validation, Visualization, Writing – original draft, Writing – review & editing. **Daniela Krentz:** Resources, Writing – review & editing. **Katharina Zwicklbauer:** Resources, Writing – review & editing. **Katrin Hartmann:** Conceptualization, Resources, Writing – review & editing. **Eveline Lescrinier:** Resources, Methodology, Writing – review & editing. **Martin Alberer:** Conceptualization, Writing – review & editing. **Ulrich von Both:** Conceptualization, Writing – review & editing. **Berthold Koletzko:** Conceptualization, Funding Acquisition, Resources, Writing – review &

editing.

Ethical statements

The prospective study in cats fulfilled the German guidelines for prospective studies with written informed owner consent and was approved by the Government of Upper Bavaria (Germany), reference number 55.2–2532.Vet_02–20–52 and by the ethical committee (reference number 261–19–03–2021) of the Centre for Clinical Veterinary Medicine of the LMU Munich (Munich, Germany).

Funding

Luke Tu is the recipient of a fellowship granted by the Hans-Böckler Stiftung (HBS) [414094, 2022]. This work was financially supported in part by the German Center for Child and Adolescent Health (DZKJ) [01GL2406A, 2024]. BK is the Else Kröner Seniorprofessor of Paediatrics at LMU – University of Munich, financially supported by the Charitable Else Kröner-Fresenius-Foundation (EKFZ), LMU Medical Faculty and LMU University Hospitals [No. 2020_EKSP.119, 2020].

Declaration of Competing Interest

The authors declare no conflict of interest. The HBS, EKFZ and DZKJ funding organizations were not involved in the study design, its outcome or the writing of this article.

Acknowledgements

The authors also thank Daqiang Pan (Sciex, Pharma & Life Science Research, Landwehrstrasse 54, D-64293 Darmstadt, Germany) for ZenoTOF 7600 fragmentation analysis.

Appendix A. Supporting information

Supplementary data associated with this article can be found in the online version at doi:10.1016/j.jpba.2025.116995.

References

[1] S. Paltrinieri, A. Giordano, A. Stranieri, S. Lauzi, Feline infectious peritonitis (FIP) and coronavirus disease 19 (COVID-19): are they similar? Transbound. Emerg. Dis. 68 (4) (2021) 1786–1799, https://doi.org/10.1111/tbed.13856.
[2] Y.Y. Gao, Q. Wang, X.Y. Liang, S. Zhang, D. Bao, H. Zhao, S.B. Li, K. Wang, G.X. Hu, F.S. Gao, An updated review of feline coronavirus: mind the two biotypes, Virus Res 326 (2023) 199059, https://doi.org/10.1016/j.virusres.2023.199059.
[3] A.M. Izes, J. Yu, J.M. Norris, M. Govendir, Current status on treatment options for feline infectious peritonitis and SARS-CoV-2 positive cats, Vet. Q. 40 (1) (2020) 322–330, https://doi.org/10.1080/01652176.2020.1845917.
[4] E. Cosaro, J. Pires, D. Castillo, B.G. Murphy, K.L. Reagan, Efficacy of oral remdesivir compared to GS-441524 for treatment of cats with naturally occurring effusive feline infectious peritonitis: a blinded, non-inferiority study, Viruses 15 (8) (2023) 1680, https://doi.org/10.3390/v15081680.
[5] M. Katayama, Y. Uemura, Therapeutic effects of mutian((R)) Xraphconn on 141 client-owned cats with feline infectious peritonitis predicted by total bilirubin levels, Vet. Sci. 8 (12) (2021) 328, https://doi.org/10.3390/vetsci8120328.
[6] J. Li, Y. Chen, Y. Diao, Y. Su, Q. Wang, Z. Yao, T. Yi, W. Jin, D. Zhao, C. Wang, M. Liu, H. Liu, Identification of metabolites of the novel anti-tumor drug candidate MDH-7 in rat urine by liquid chromatography coupled with triple quadrupole linear ion trap mass spectrometry, Rapid Commun. Mass Spectrom. 30 (7) (2016) 1001–1010, https://doi.org/10.1002/rcm.7506.
[7] H.M. Lee, B.J. Lee, A novel approach to simultaneous screening and confirmation of regulated pharmaceutical compounds in dietary supplements by LC/MS/MS with an information-dependent acquisition method, Food Addit. Contam.: Part A 28 (4) (2011) 396–407, https://doi.org/10.1080/19440049.2011.551947.
[8] M. Yao, L. Ma, W.G. Humphreys, M. Zhu, Rapid screening and characterization of drug metabolites using a multiple ion monitoring-dependent MS/MS acquisition method on a hybrid triple quadrupole-linear ion trap mass spectrometer, J. Mass Spectrom. 43 (10) (2008) 1364–1375, https://doi.org/10.1002/jms.1412.
[9] S. Dresen, N. Ferreiros, H. Gnann, R. Zimmermann, W. Weinmann, Detection and identification of 700 drugs by multi-target screening with a 3200 Q TRAP LC-MS/MS system and library searching, Anal. Bioanal. Chem. 396 (7) (2010) 2425–2434, https://doi.org/10.1007/s00216-010-3485-2.
[10] L. Kortz, R. Geyer, U. Ludwig, M. Planert, M. Bruegel, A. Leichtle, G.M. Fiedler, J. Thiery, U. Ceglarek, Simultaneous eicosanoid profiling and identification by liquid chromatography and hybrid triple quadrupole-linear ion trap mass spectrometry for metabolomic studies in human plasma, LaboratoriumsMedizin 33 (6) (2009) 341–348, https://doi.org/10.1515/jlm.2009.057.
[11] P.J. Heinsvig, C. Noble, P.W. Dalsgaard, M. Mardal, Forensic drug screening by liquid chromatography hyphenated with high-resolution mass spectrometry (LC-HRMS), TrAC Trends Anal. Chem. 162 (2023) 117023, https://doi.org/10.1016/j.trac.2023.117023.
[12] H.P. Benton, J. Ivanisevic, N.G. Mahieu, M.E. Kurczy, C.H. Johnson, L. Franco, D. Rinehart, E. Valentine, H. Gowda, B.K. Ubhi, R. Tautenhahn, A. Gieschen, M. W. Fields, G.J. Patti, G. Siuzdak, Autonomous metabolomics for rapid metabolite identification in global profiling, Anal. Chem. 87 (2) (2015) 884–891, https://doi.org/10.1021/ac5025649.
[13] Z. Zhou, M. Luo, X. Chen, Y. Yin, X. Xiong, R. Wang, Z.J. Zhu, Ion mobility collision cross-section atlas for known and unknown metabolite annotation in untargeted metabolomics, Nat. Commun. 11 (1) (2020) 4334, https://doi.org/10.1038/s41467-020-18171-8.
[14] A. Helms, E.E. Escobar, S. Vainauskas, C.H. Taron, J.S. Brodbelt, Ultraviolet photodissociation permits comprehensive characterization of O-glycopeptides cleaved with O-glycoprotease IMPa, Anal. Chem. 95 (24) (2023) 9280–9287, https://doi.org/10.1021/acs.analchem.3c01111.
[15] T. Baba, P. Ryumin, E. Duchoslav, K. Chen, A. Chelur, B. Loyd, I. Chernushevich, Dissociation of biomolecules by an intense low-energy electron beam in a high sensitivity time-of-flight mass spectrometer, J. Am. Soc. Mass Spectrom. 32 (8) (2021) 1964–1975, https://doi.org/10.1021/jasms.0c00425.
[16] T. Baba, Z. Zhang, S. Liu, L. Burton, P. Ryumin, J.C.Yves Le Blanc, Localization of multiple O-linked glycans exhibited in isomeric glycopeptides by hot electron capture dissociation, J. Proteome Res. 21 (10) (2022) 2462–2471, https://doi.org/10.1021/acs.jproteome.2c00378.
[17] U. Holzgrabe, M. Malet-Martino, Analytical challenges in drug counterfeiting and falsification-The NMR approach, J. Pharm. Biomed. Anal. 55 (4) (2011) 679–687, https://doi.org/10.1016/j.jpba.2010.12.017.
[18] K. Habler, M. Bruegel, D. Teupser, U. Liebchen, C. Scharf, U. Schoenermarck, M. Vogeser, M. Paal, Simultaneous quantification of seven repurposed COVID-19 drugs remdesivir (plus metabolite GS-441524), chloroquine, hydroxychloroquine, lopinavir, ritonavir, favipiravir and azithromycin by a two-dimensional isotope dilution LC-MS/MS method in human serum, J. Pharm. Biomed. Anal. 196 (2021) 113935, https://doi.org/10.1016/j.jpba.2021.113935.
[19] B. Kimble, S.J. Coggins, J.M. Norris, M.F. Thompson, M. Govendir, Quantification of GS-441524 concentration in feline plasma using high performance liquid chromatography with fluorescence detection, Vet. Q. 43 (1) (2023) 1–9, https://doi.org/10.1080/01652176.2023.2246553.
[20] J.C. Alvarez, P. Moine, I. Etting, D. Annane, I.A. Larabi, Quantification of plasma remdesivir and its metabolite GS-441524 using liquid chromatography coupled to tandem mass spectrometry. Application to a Covid-19 treated patient, Clin. Chem. Lab. Med. 58 (9) (2020) 1461–1468, https://doi.org/10.1515/cclm-2020-0612.
[21] V. Avataneo, A. de Nicolo, J. Cusato, M. Antonucci, A. Manca, A. Palermiti, C. Waitt, S. Walimbwa, M. Lamorde, G. di Perri, A. D'Avolio, Development and validation of a UHPLC-MS/MS method for quantification of the prodrug remdesivir and its metabolite GS-441524: a tool for clinical pharmacokinetics of SARS-CoV-2/COVID-19 and Ebola virus disease, J. Antimicrob. Chemother. 75 (7) (2020) 1772–1777, https://doi.org/10.1093/jac/dkaa152.
[22] D. Krentz, K. Zenger, M. Alberer, S. Felten, M. Bergmann, R. Dorsch, K. Matiasek, L. Kolberg, R. Hofmann-Lehmann, M.L. Meli, A.M. Spiri, J. Horak, S. Weber, C. M. Holicki, M.H. Groschup, Y. Zablotski, E. Lescrinier, B. Koletzko, U. von Both, K. Hartmann, Curing Cats with Feline Infectious Peritonitis with an Oral Multi-Component Drug Containing GS-441524, Viruses 13 (11) (2021), https://doi.org/10.3390/v13112228.
[23] J. Schleucher, M. Schwendinger, M. Sattler, P. Schmidt, O. Schedletzky, S.J. Glaser, O.W. Sorensen, C. Griesinger, A general enhancement scheme in heteronuclear multidimensional NMR employing pulsed field gradients, J. Biomol. NMR 4 (2) (1994) 301–306, https://doi.org/10.1007/BF00175254.
[24] J. Ruiz-Cabello, G.W. Vuister, C.T.W. Moonen, P. van Gelderen, J.S. Cohen, P.C. M. van Zijl, Gradient-enhanced heteronuclear correlation spectroscopy. Theory and experimental aspects, J. Magn. Reson. (1969) 100 (2) (1992) 282–302, https://doi.org/10.1016/0022-2364(92)90262-6.
[25] B.K. Matuszewski, M.L. Constanzer, C.M. Chavez-Eng, Strategies for the assessment of matrix effect in quantitative bioanalytical methods based on HPLC-MS/MS, Anal. Chem. 75 (13) (2003) 3019–3030, https://doi.org/10.1021/ac020361s.
[26] European Medicines Agency, Guideline on Bioanalytical Method Validation, (2011). ⟨https://www.ema.europa.eu/en/documents/scientific-guideline/guideline-bioanalytical-method-validation_en.pdf⟩ (accessed 22 May 2025).
[27] F. Allen, A. Pon, M. Wilson, R. Greiner, D. Wishart, CFM-ID: a web server for annotation, spectrum prediction and metabolite identification from tandem mass spectra, Nucleic Acids Res 42 (W1) (2014) W94–W99, https://doi.org/10.1093/nar/gku436.
[28] M.O.N.H. Clarke, E. Doerffler, R.L. Mackman, D. Siegel, Pyrrolo[1,2-f][1,2,4] Triazines Useful for Treating Respiratory Syncytial Virus Infections. Gilead Sciences, Inc.; 333 Lakeside Drive, Foster City, CA 94404, USA assignee. Patent WO2015069939A1. 2015.
[29] M.J. Perron, Methods of treating feline coronavirus infections. Gilead Sciences, Inc.; USA assignee. Patent WO2018169946A1. 2018.
[30] H. Hu, S. Zhang, Nucleosides salt and preparation method thereof. Jinan Mutian Biotechnology Co., Ltd. assignee. Patent WO2021022690A1. 2021.

[31] M. Hu, D. Hong, W. Xue, W. A kind of nucleoside compound containing six-membered ring and preparation method thereof. Nantong Weishun Biotechnology Co., Ltd. assignee. Patent CN111454270A. 2020.
[32] M. Hu, D. Hong, W. Xue, W. Six-membered ring-containing nucleoside compound and preparation method thereof. Nantong Weishun Biotechnology Co Ltd assignee. Patent US10988503B1. 2021.
[33] T.K. Warren, R. Jordan, M.K. Lo, A.S. Ray, R.L. Mackman, V. Soloveva, D. Siegel, M. Perron, R. Bannister, H.C. Hui, et al., Therapeutic efficacy of the small molecule GS-5734 against Ebola virus in rhesus monkeys, Nature 531 (7594) (2016) 381–385, https://doi.org/10.1038/nature17180.
[34] Q. Chen, Q. Zhou, G. Li, S. Li, Y. Li, X. Zhang, Optimized Kilogram-Scale Synthesis and Impurity Identification of SHEN26 (ATV014) for Treating COVID-19, Org. Process Res. Dev. 28 (6) (2023) 2188–2195, https://doi.org/10.1021/acs.oprd.3c00248.
[35] M. Tempestilli, P. Caputi, V. Avataneo, S. Notari, O. Forini, L. Scorzolini, L. Marchioni, T. Ascoli Bartoli, C. Castilletti, E. Lalle, M.R. Capobianchi, E. Nicastri, A. DÁvolio, G. Ippolito, C. Agrati, Pharmacokinetics of remdesivir and GS-441524 in two critically ill patients who recovered from COVID-19, J. Antimicrob. Chemother. 75 (10) (2020) 2977–2980, https://doi.org/10.1093/jac/dkaa239.